Dynamics of NO rebinding to the heme domain of NO synthase-like proteins from bacterial pathogens

ARTICLE *in* NITRIC OXIDE · JANUARY 2007

Impact Factor: 3.52 · DOI: 10.1016/j.niox.2006.03.010 · Source: PubMed

Available online at www.sciencedirect.com
ScienceDirect
Nitric Oxide 15 (2006) 312–327
NITRIC OXIDE Biology and Chemistry
www.elsevier.com/locate/yniox

Dynamics of NO rebinding to the heme domain of NO synthase-like proteins from bacterial pathogens

Clément Gautier [a,b], Ivan Mikula [c], Pierre Nioche [d], Pavel Martasek [c], C.S. Raman [d], Anny Slama-Schwok [a,b,*]

[a] *CNRS, UMR 7645, Laboratory of Optics and Biosciences, Ecole Polytechnique, 91128 Palaiseau, France*
[b] *Inserm, U696, F-91128 Palaiseau, France*
[c] *Department of Pediatrics, First School of Medicine, Charles University of Prague, Czech Republic*
[d] *Department of Biochemistry and Molecular Biology, University of Texas Medical School, Houston, Texas, USA*

Received 1 November 2005; revised 24 February 2006
Available online 5 April 2006

Abstract

Some Gram-positive bacterial pathogens harbor a gene that encodes a protein (HNS, Heme domain of NO Synthase-like proteins) with striking sequence identity to the oxygenase domain of mammalian NO synthases (NOS). However, they lack the N-terminal and the Zn-cysteine motif participating to the stability of an active dimer in the mammalian isoforms. The unique properties of HNS make it an excellent model system for probing how the heme environment tunes NO dynamics and for comparing it to the endothelial NO synthase heme domain ($eNOS_{HD}$) using ultrafast transient spectroscopy. NO rebinding in HNS from *Staphylococcus aureus* (SA-HNS) is faster than that measured for either *Bacillus anthracis* (BA-HNS) or for $eNOS_{HD}$ in both oxidized and reduced forms in the presence of arginine. To test whether these distinct rates arise from different energy barriers for NO recombination, we measured rebinding kinetics at several temperatures. Our data are consistent with different barriers for NO recombination in SA-HNS and BA-HNS and the presence of a second NO-binding site. The hypothesis that an additional NO-binding cavity is present in BA-HNS is also consistent with the effect of the NO concentration on its rebinding. The lack of the effect of NO concentration on the geminate rebinding in SA-HNS could be due to an isolated second site. We confirm the existence of a second NO site in the oxygenase domain of the reduced eNOS as previously hypothesized [A. Slama-Schwok, M. Négrerie, V. Berka, J.C. Lambry, A.L. Tsai, M.H. Vos, J.L. Martin, Nitric oxide (NO) traffic in endothelial NO synthase. Evidence for a new NO binding site dependent on tetrahydrobiopterin? J. Biol. Chem. 277 (2002) 7581–7586]. This site requires the presence of arginine and BH_4; and we propose that NO dynamic and escape from eNOS is regulated by the active site H-bonding network connecting between the heme, the substrate, and cofactor.

Keywords: Endothelial NO-synthase; Heme domain; Bacterial NOS-like proteins; Ultrafast kinetics; Geminate; Rebinding of NO; Arginine; Tetrahydrobiopterin

Introduction

In mammals, nitric oxide (NO) is biosynthesized from L-arginine by three isoforms of nitric oxide synthases (NOS) and goes on to function as a signalling molecule that mediates a plethora of cellular activities including vascular homeostasis, neurotransmission, and host defense [1]. NO signalling is not confined to the animal kingdom, NO participates in plant development and defense responses [2]. Some bacteria (denitrifying organisms) retain the capability to generate NO while respiring on nitrate and nitrite [3]. Non-denitrifiers like *Escherichia coli* produce NO during anaerobic nitrate respiration [4]. Recently, Zumft [5] provided evidence that NO can also function as a signalling molecule in prokaryotes opening new avenues to explore.

Since the discovery and cloning of mammalian NOS [6], several reports suggested that bacteria contained a

* Corresponding author. Fax: +33 1 69333017.
E-mail address: anny.schwok@polytechnique.fr (A. Slama-Schwok).

1089-8603/$ - see front matter © 2006 Elsevier Inc. All rights reserved.
doi:10.1016/j.niox.2006.03.010

NOS-like protein [for a review, see 7]. Nitric oxide synthases-like proteins from several bacterial strains were first identified in *Nocardia* [8], in *Lactobacillus fermentum* [9], *Staphylococcus aureus* [10] and more recently in *Bacillus subtilis* [11–13], *Deinococcus radiodurans* [14], and *S. aureus* [15]. Several reports showed that purified HNS in vitro are capable of generating NO via monoxygenation reactions when artificially linked to mammalian di-flavin reductase domain [16–18]. Bacterial NOS-like proteins from *Streptomyces* and *D. radiodurans* nitrate small molecules such as tryptophan and a related compound [16,18,19]. Nevertheless, the function of these proteins in a physiological setting is incompletely understood.

In the following, we use "HNS" (heme domain of a nitric oxide synthase-like protein) to designate the bacterial proteins. The HNS proteins revealed a high homology with the oxygenase domain of the mammalian NOS, despite the lack of the N-terminal domain with the Zn-cysteines motif that helped in the formation of an active dimer in the mammalian NOS and the C-terminal di-flavin reductase domain. Of specific interest was the total absence of a di-flavin reductase (with the exception of sulfite reductase) in *D. radiodurans*. The cloning, spectroscopic characterization, and the ability to generate diffraction-quality crystals from *S. aureus* and *Bacillus anthracis* was reported in 2001 [20,21] and structures of *B. subtilis* [11] and *S. aureus* [15] were published in 2002. These structures reveal that the HNS, although presenting subtle sequence changes in the heme pocket, adopt a very similar conformation in the heme vicinity when compared to the mammalian NOS. Thus, the bacterial proteins provide a model system to better understand the inner-workings of mammalian NOS. Recombination of NO ligand after photodissociation is an adequate tool to probe heme conformations within these bacterial proteins and compared them with the oxygenase domain of the endothelial NO-synthase $eNOS_{HD}$, with high relevance to mammalian NOS regulation [22,23].

Geminate recombination, a powerful tool to study NOS molecular regulation

The activity of NOS proteins is differently regulated at the level of their nitrosyl complexes: the ferrous heme–NO complex governs and limits the rate of NO synthesis in nNOS [24,25]. In contrast, the ferric nitrosyl complex regulates iNOS catalysis [24]. The regulation of NOS proteins by their nitrosyl complexes is controlled by the bimolecular rate of NO binding to the protein, k_{on}, leading to a tighter regulation as NO accumulates in the medium. It also depends on the (monomolecular) dissociation rate of NO from the protein, k_{off}.

Our experiments probe the fast intramolecular recombination of NO with the heme, a step controlling both k_{on} and k_{off} rates. We use a pump pulse at correct wavelength (565 nm), that cleaves selectively the heme Fe—NO bond of the ferric (or ferrous) nitrosyl complex within 30 fs. A probe beam monitors the absorption changes consecutive to this bond break. It results in the formation of a ferric (or ferrous) unliganded heme and photodissociated NO located in the vicinity of the heme and in the heme pocket. The subsequent rebinding of NO to the heme is followed by the changes in the optical absorption as a function of time. The process of reformation of the ferric (or ferrous) nitrosyl complex (after photodissociation of the heme ligand) is called geminate recombination. The intensity of the geminate recombination signal is given by the difference between Fe(III) and Fe(III)-NO absorption in the case of the ferric nitrosyl complex; at zero signal, all the NO rebound to the heme. Since these kinetics are recorded in the fs to ns time scale, only intramolecular processes of NO diffusion within the protein are followed. Diffusion of NO from the solution would occur at much slower time scales (μs to ms).

The geminate recombination is often a multi-phasic process [26–28]. This process involves a picosecond step due to the rebinding of NO that did not escape the heme vicinity after photodissociation and is probably activationless. The nanosecond step phase reflects the rebinding of NO molecules dissociated with excess energy from the protein to the heme pocket but still remaining in the protein. The latter step is generally associated with overcoming of internal energy barrier(s), alternatively assigned to ligand migration [28,29]. The upper limit of the probability of NO escape from the protein is given by the asymptotic value, corresponding to NO ligands remaining unbound in 3–5 ns.

In the present work, we compare the dynamics of NO rebinding to the heme in two bacterial enzymes and the oxygenase domain of the endothelial NOS, using ultrafast transient absorption spectroscopy. The bacterial proteins from *S. aureus* and *B. anthracis* allowed comparing subtle sequence changes in the heme pocket and their influence on NO dynamics by comparison with the heme domain of mammalian eNOS, $eNOS_{HD}$.

When arginine was present, we found that the rates of NO rebinding in SA-HNS were always faster than that in either BA-HNS or $eNOS_{HD}$ in their oxidized and reduced forms. To identify the origin of these kinetic variations, the effect of the temperature on NO rebinding in both SA-HNS and BA was determined: the rationale being that a higher rebinding rate in SA-HNS compared to BA-HNS could reflect different energy barriers for NO recombination to the heme in the two proteins. Our findings are consistent with a free diffusion of NO in the heme pocket of BA-HNS and $eNOS_{HD}$, in agreement with a previous report [23]. Thus, NO escapes easily from these proteins, without limitation of large energy barriers, provided that arginine is present. In contrast, NO is "trapped" in SA-HNS. The probability of NO escape is small at low temperature but can be increased by raising the temperature, in agreement with the existence of internal energy barriers. NO release from $eNOS_{HD}$ seems to be controlled by the H-bonding network linking the substrate, NO, the cofactor and the heme [7]. We identify distinct interactions

between a conserved arginine and the heme propionates in the three proteins that may explain the kinetic measurements.

Experimental

Materials

L-Arginine, (6R)5,6,7,8-tetrahydrobiopterin (BH_4), as well as chemicals used for the Tris–HCl buffer, sodium dithionite, potassium ferricyanide, glycerol were purchased from Sigma. Certified dilutions of NO gas at 0.1%, 1% or 10% in argon and high purity argon (99.9995%) were obtained from Alpha Gaz.

Expression of the enzymes

HNS from *S. aureus* (SA), *B. anthracis* (BA), and eNOS oxygenase domain ($eNOS_{HD}$) were over-expressed in *E. coli* and purified as reported previously [7,30].

Preparation of samples for spectroscopy

A concentrated solution of proteins (at a final concentration of 70–100 μM) in 50 mM Tris–HCl buffer containing 150 mM NaCl at pH = 7.5 and 5% glycerol was mixed with 2.0 mM arginine in a optical cuvette with a 1 mm path length. The cell was sealed with a rubber stopper and degassed by repetitive cycles of vacuum and argon. Freshly prepared solutions of tetrahydrobiopterin (BH_4) under argon were added to a deaerated eNOS solution at the final concentration of 200 μM when BH_4-repleted samples were needed. The concentration of BH_4 was determined by its absorbance at 298 nm ($\varepsilon_{298} = 9.4 \times 10^3\,M^{-1}\,cm^{-1}$) measured at pH = 7.5 and was found to be similar to the reported value [31]. NO gas was then introduced in the cell at a pressure of 1.3 bar using a gas train. Reduction of the samples was achieved using a slight molar excess of dithionite solution (that was previously titrated with potassium ferricyanide).

Time-resolved spectroscopy

Time-resolved spectroscopy was performed with a 30 Hz pump-probe laser set-up described previously [32]. Photodissociation of NO-bound HNS and $eNOS_{HD}$ was achieved by an excitation pulse at 565 nm with a pulse width of 40 fs. The transient spectrum detected after a variable delay was probed with a white light continuum pulse, whose group velocity dispersion was minimized at 400 nm by a set of prisms. The wavelength calibration of the CCD camera was checked daily by using a narrow-band filter. Twenty-five scans were recorded in a single experiment in three time windows: 50, 500 ps, and 3 ns. Carbon monoxide bound to reduced myoglobin was monitored under the same conditions and used as a reference of flat kinetics in the time scales of 500 ps to 4 ns [32]. Analysis of the data was performed by singular matrix decomposition (SVD) of the time-wavelength matrix [33].

Effect of temperature

The temperature of the cell holder was regulated by circulating water from a temperature-controlled bath. Nitrogen was blown on the cuvettes to avoid water condensation at low temperatures. Experiments were performed once by increasing the temperature from 9 to 30 °C and in reverse to check for reproducibility. No more than three kinetics traces were recorded with a single protein sample. The optical spectra after the laser experiments reveal that some proteins became deliganded, especially in BA-HNS at high temperature. The solution was then re-equilibrated with 0.1% NO and the absorption spectrum was recorded again and compared to a spectrum taken before the laser experiment to verify that the protein had not denatured. Heating above 33 °C resulted in the onset of precipitation. The fitted data (to two exponentials and a constant) have been calculated according to two models based on Scheme 1. Scheme 1 defines four rate constants: $k1$ is the rate of NO rebinding from N to H, $k2$ from S to N, $k3$ from O to S as well as reverse rates; k-2 from N to S and k-3 from S to O. Two models were tested. In the first model, it is assumed that there is no contribution of ligands from the solution to NO rebinding; the second model assumes that there could be some contribution from the bulk. Details of the calculations are given in Appendix A. Activation parameters were obtained from the temperature dependence of each calculated rate ki, using the Eyring equation [34]: $\Delta G^{\#}/T = R \ln[(k_B T/h)(1/ki)]$, where $R = 2\,cal\,K^{-1}\,mol^{-1}$, $k_B = 1.38 \times 10^{-16}\,erg\,K^{-1}$, $h = 6.626 \times 10^{-27}\,erg\,s$ and T is the temperature in Kelvin. The plot of $\Delta G^{\#}/T$ as a function of $1/T$ yields the activation parameters (recall that $\Delta G^{\#}/T = \Delta H^{\#}(1/T) - \Delta S^{\#}$).

Results

Geminate recombination of NO to the ferric enzymes; effect of L-arginine

Fig. 1 shows the transient spectra obtained 30 ps after NO photodissociation from the ferric nitrosyl complex of BA-HNS in the presence or absence of arginine. Both spectra are super imposable (Fig. 1, left panel), characterized by a positive peak at 396 nm and a negative minimum at 441 nm. In contrast, the equilibrium difference spectra between the unliganded ferric heme and Fe(III)-NO differ when arginine is present or absent, by a red-shift from 397 to 401 nm respectively (Fig. 1, right panel). This shift to 401 nm shows that BA-HNS contained some low spin species in the absence of arginine. Since the transient spectra are identical within experimental error with or without arginine and present the same maxima as the equilibrium difference in the presence of arginine, our experiment only monitors NO geminate recombination to the high spin

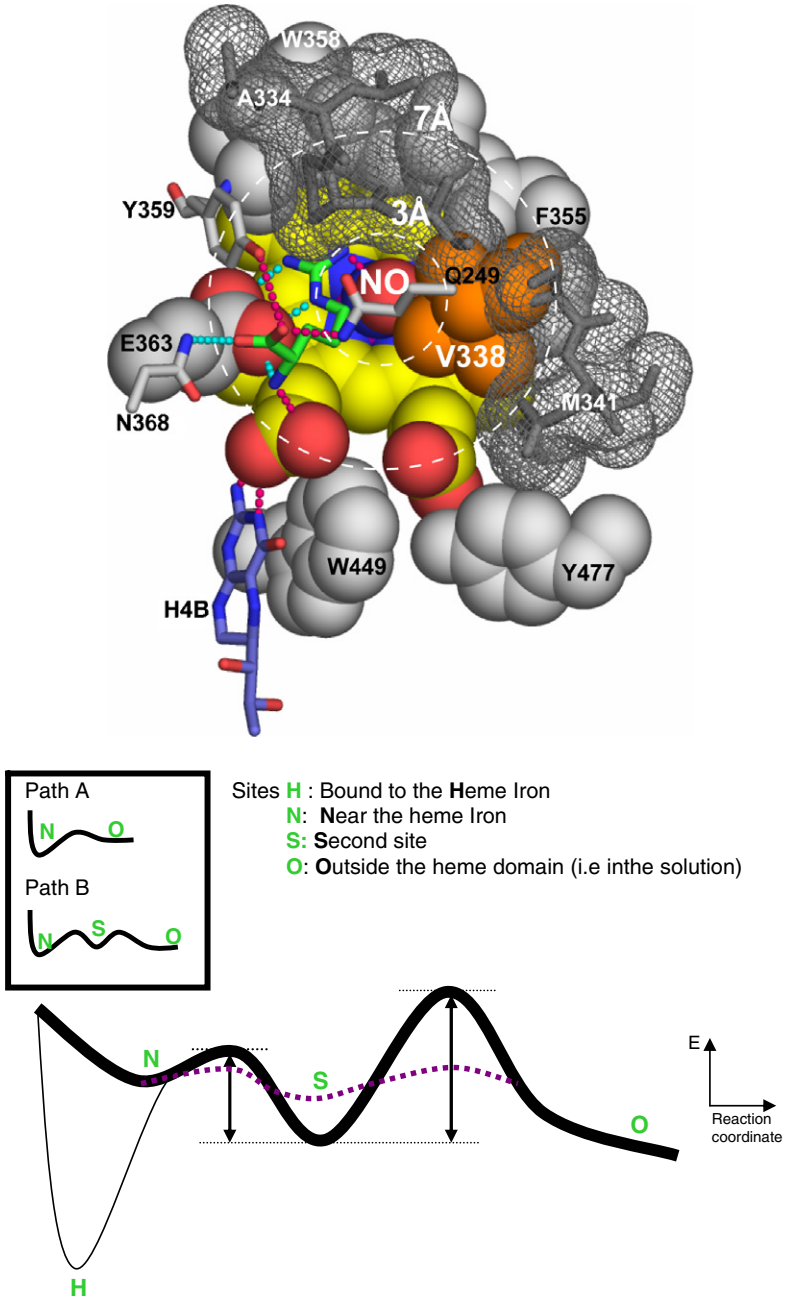

Scheme 1. Bottom: Energy diagrams for the bacterial HNS BA and SA proteins: N stands for the ferrous unliganded heme, H: NO-liganded heme, S: a second site in the protein, 0: exterior of the protein (solution); the black full line corresponds to SA-HNS, the purple dotted line to BA-HNS; the relevant energy barriers according to models 1 and 2 are highlighted by arrows. Up: H-bonding network in $eNOS_{HD}$ that control NO release: The heme plane is represented in yellow balls with propionate oxygens in red; NO is represented in blue and red balls; the aromatic residues defining the edge of the heme pocket are shown in grey; Val338 is represented in brown balls, the aliphatic amino acids next to Val338 and the residues forming H-bonds with the heme are shown in grey sticks colored in blue or red in the presence of N or O atoms, with the H-bonds schematised as thick dotted lines [6], the substrate arginine (green) and the cofactor BH_4 (violet) are shown in sticks. The circles highlights distances of 3 Å (heme site) and 7 Å, area including the second NO site. (For interpretation of the references to color in this figure legend, the reader is referred to the web version of this paper.)

ferric heme. The same holds true for $eNOS_{HD}$ and SA-HNS (data not shown).

The kinetics of NO rebinding to the heme in SA, BA-HNS, and $eNOS_{HD}$ is shown in Fig. 2 in the absence (A) and presence of arginine (B). The geminate recombination of NO to BA-HNS in the absence of arginine is best fitted by three exponentials with time constants $\tau_1 = (29 \pm 5)$ ps, $\tau_2 = (287 \pm 40)$ ps, $\tau_3 = (1883 \pm 250)$ ps and a very small constant term. NO rebinding to SA-HNS and to BA-HNS present very similar kinetics, especially in the first 50 ps as shown in Fig. 2A and Table 1, when arginine is absent. This similarity between the two HNS contrasts with NO rebinding to $eNOS_{HD}$, characterized by a much slower picosecond component $\tau_1 = (111 \pm 20)$ ps.

The similarity between the two HNS no longer holds in the presence of arginine (Fig. 2B). NO rebinding to

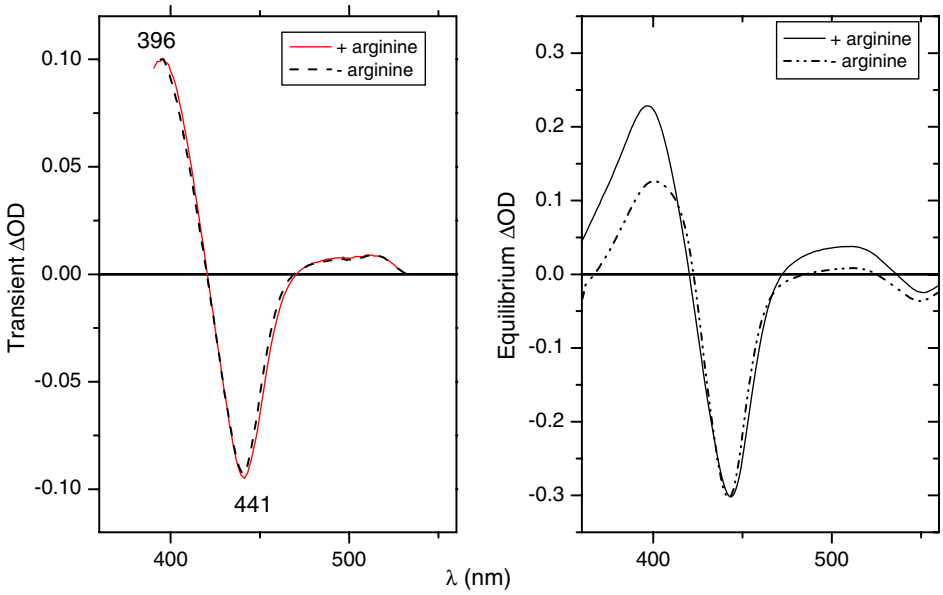

Fig. 1. Effect of the substrate on the equilibrium and transient difference absorption spectra Fe(III)–Fe(III)-NO of the bacterial BA-HNS. Left: transient difference spectra recorded in the presence of L-arginine are full lines and without arginine are dashed lines. Right: equilibrium difference spectra recorded in the presence (full line) or absence of arginine (broken lines). [BA-HNS] = 70 μM, 50 mM Tris buffer at pH = 7.5, 150 mM NaCl, 5% glycerol, 10% NO in the gas phase.

SA-HNS is now characterized by a large amplitude $A_1 = 0.54$ of the short component $\tau_1 = (50 \pm 5)$ ps and a large constant term $A_4 = 0.30$. Thus, part of the NO rebinds faster but also more NO escapes rebinding in SA-HNS in the presence of arginine as compared to that without. These effects are independent of the NO concentration, 1 or 10% in the gas phase (Table 1). Similar kinetics is obtained in the presence of tetrahydrofolate (data not shown). NO recombination in BA-HNS becomes similar to that in $eNOS_{HD}$ when arginine is present. Both τ_1 and τ_2 become faster upon arginine binding, whereas τ_3 remains similar within experimental error. This effect is partly balanced by smaller amplitudes of the first exponent: A_1 decreases from 0.30 to 0.09 and from 0.21 to 0.10 in BA-HNS and $eNOS_{HD}$, respectively, without and with arginine. Arginine also modifies the recombination in the nanosecond regime as attested by the large amplitude of A_4 (Table 1). Thus, the probability that NO escapes geminate recombination increases in the presence of arginine as reported for the entire eNOS [23,30] and shared with the bacterial HNS.

NO geminate rebinding to the ferrous enzymes: probing internal energy barriers by the effect of temperature on NO rebinding to the heme

Fig. 2B clearly showed that NO rebinding in SA-HNS is faster than in either BA-HNS or $eNOS_{HD}$ in the presence of arginine. The following experiments were designed to test whether this comparison holds true for HNS in their reduced form and could be characteristic of these proteins.

The kinetics of NO rebinding in the three reduced proteins in the presence of arginine are presented in Fig. 3 and summarized in Table 2. The rebinding kinetics of NO in SA-HNS is characterized by a major contribution of a short lifetime $\tau_1 = (13 \pm 2)$ ps with a similar amplitude as that found in the oxidized form, $A_1 = 0.50$. The second exponent is $\tau_2 = (175 \pm 50)$ ps, whereas the third term is longer or equal to 3 ns and may be included in the constant term. In contrast, the amplitude of the first lifetime is much smaller in both BA-HNS and $eNOS_{HD}$, $A_1 = 0.18$ and 0.17, respectively. However, A_4 do not largely differ, $A_4 = 0.26$, 0.25, and 0.13 for SA-HNS, $eNOS_{HD}$, and BA-HNS, respectively.

Figs. 2B and 3 clearly indicate that NO rebinding in SA-HNS is significantly faster than in either BA-HNS or $eNOS_{HD}$, both in their oxidized and reduced forms. This appears to be characteristic of SA-HNS and could arise from different energy barriers for NO rebinding to the heme as compared to BA-HNS. This energy barrier for NO may separate the heme from the solution (path A; see Scheme 1). If excess thermal energy is supplied to the dissociated NO by heating, these ligands could more easily cross over this barrier from the heme to the protein exterior and vice versa. Thus, the recombination rates should increase. Alternatively, path B considers that energy barriers have to be crossed over in order to reach a second NO site from the heme (or heme pocket) and vice versa. Thus, one expects a higher probability of populating a second site with an increase of the temperature. If the second site itself is separated from the solution by another barrier, then the global effect of raising the temperature would be to decrease the extent of recombination and increase of NO escape. We thus performed NO rebinding experiments in both HNS as a function of temperature.

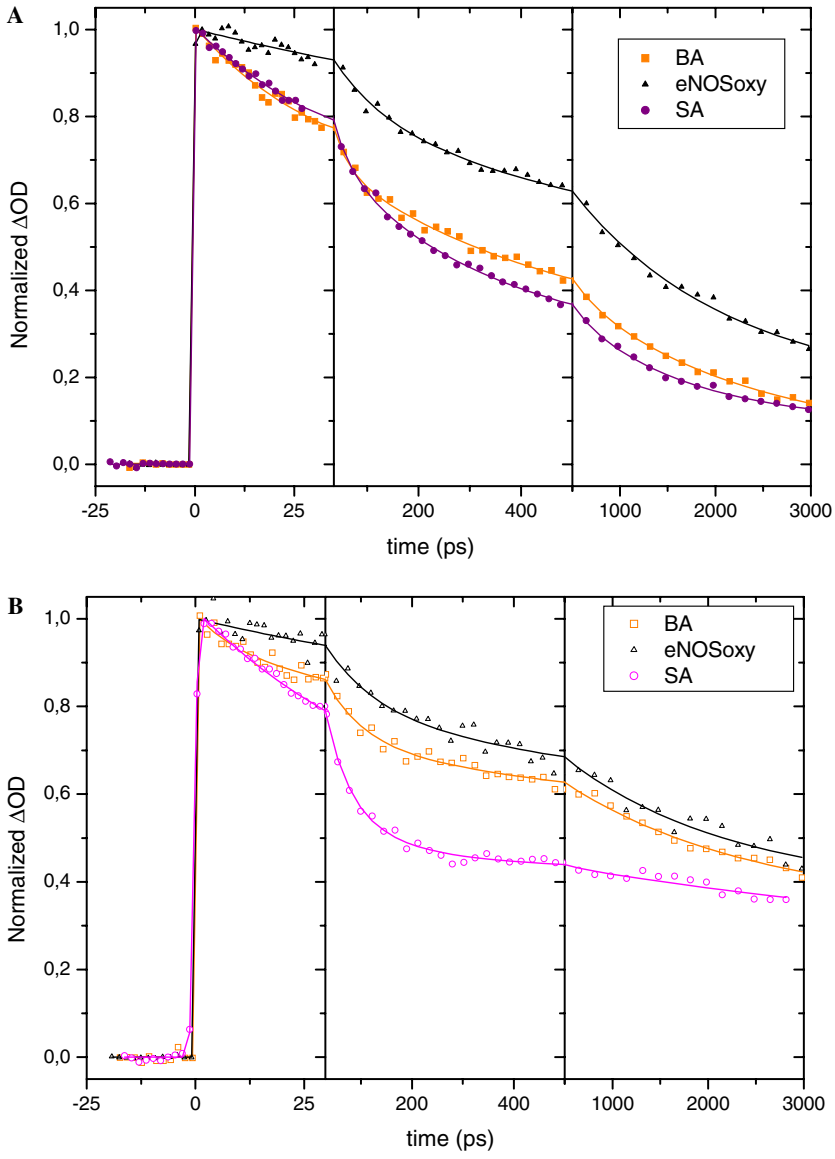

Fig. 2. Comparison of NO geminate recombination in the oxidized bacterial HNS SA and BA compared to eNO_{SHD} at 10% NO. (A) In the absence of arginine: ■, BA-HNS; ▲, $eNOS_{HD}$; ●, SA-HNS. (B) In the presence of arginine: □, BA-HNS; △, $eNOS_{HD}$; ○, SA-HNS. [protein] = (70–100) μM, same conditions as in Fig. 1.

Table 1
Kinetic parameters obtained from the ferric $eNOS_{HD}$, BA-, and SA-HNS

Protein	Arginine	BH_4	[NO] (%)	A_1[a] (ps)	τ_1	A_2[a] (ps)	τ_2	A_3[a] (ps)	τ_3	A_4[a]
BA	0	–	10	0.30	29	0.24	287	0.405	1883	0.05
BA	+	–	10	0.09	9	0.36	81	0.33	2014	0.33
SA	0	–	1	0.25	30	0.32	207	0.34	1452	0.09
SA	0	–	10	0.26	34	0.29	214	0.36	1273	0.09
SA	+	–	1	0.56	54	—	—	0.14	1000	0.30
SA	+	–	10	0.53	48	—	—	0.16	850	0.31
$eNOS_{HD}$	0	+	10	0.21	111	—	—	0.62	1677	0.17
$eNOS_{HDHD}$	+	+	10	0.10	58	0.14	200	0.40	2500	0.35

Parameters obtained by fitting the kinetics associated with the main SVD component (SVD1) [eNOS] = [SA-HNS] = [BA-HNS] = (70–100) μM, 50 mM Tris buffer at pH = 7.5 containing 150 mM NaCl and 5% glycerol, 2 mM arginine represented by '+' in the arginine column, 200 μM BH_4 added: + in the BH_4 column; no arginine added: 0.

[a] Relative amplitude, $A_1 + A_2 + A_3 + A_4 = 1$, not including the amplitude of the transient due to the excited state. In order to allow a better comparison, the main SVD components have been arbitrary normalized to 1.

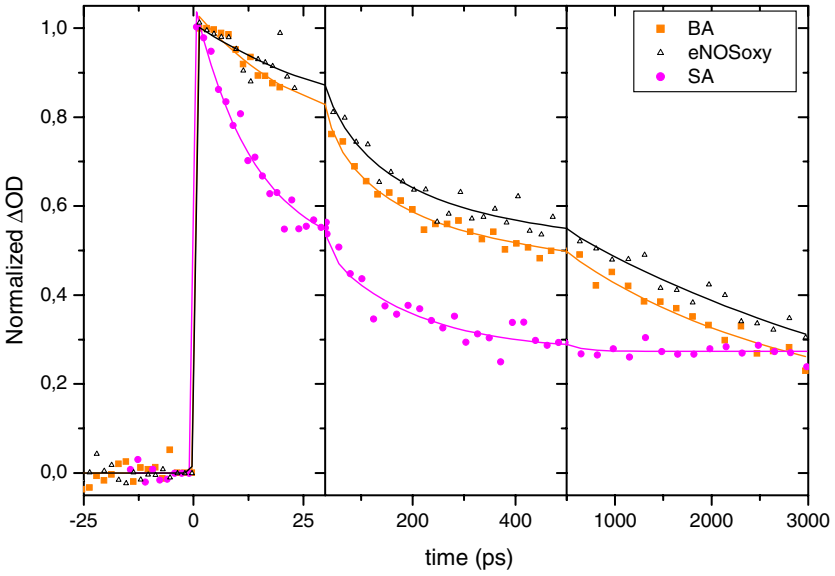

Fig. 3. Comparison of NO rebinding in the three reduced NOS proteins using [NO] = 0.1%. SA-HNS, ●; BA-HNS, ■; $eNOS_{HD}$ in the presence of BH_4, ▲. [protein] = (70–100) μM, 50 mM Tris buffer at pH = 7.5, 150 mM NaCl, 5% glycerol, 2 mM arginine, 0.1% NO in the gas phase.

Table 2
Kinetic parameters obtained from the ferrous $eNOS_{HD}$, BA-, and SA-HNS

Protein	arginine	BH_4	[NO] (%)	A_1[a](ps)	τ_1	A_2[a] (ps)	τ_2	A_3[a] (ps)	τ_3	A_4[a]
BA	+	–	0.02	0.15	102	—	—	0.45	1718	0.40
BA	+	–	0.055	0.32	17	0.35	551	—	—	0.33
BA	+	–	0.1	0.18	19	0.24	114	0.49	2411	0.13
BA	+	–	1	0.33	21	0.12	249	0.4	1960	0.15
SA	+	–	0.04	0.51	15	0.27	226	—	—	0.22
SA	+	–	0.1	0.50	13	0.24	175	—	—	0.26
SA	+	–	1	0.45	12	0.24	98	0.31	2765	0
$eNOS_{HD}$	+	+	0.1	0.11	26	0.28	126	0.61	4325	0
$eNOS_{HD}$	+	+	1	0.45	25	0.19	337	0.29	2978	0.07
$eNOS_{HD}$	+	–	0.1	0.17	72	—	—	0.58	2788	0.25
$eNOS_{HD}$	+	–	1	0.21	41	—	—	0.56	3284	0.23
$eNOS_{HD}$	–	+	0.1	0.27	13	0.34	87	0.17	1690	0.22
$eNOS_{HD}$	–	+	1	0.32	17	0.27	125	0.11	2120	0.30

Parameters obtained by fitting the kinetics associated with the main SVD component [eNOS] = [SA-HNS] = [BA-HNS] = (70–100) μM, 50 mM Tris buffer at pH = 7.5 containing 150 mM NaCl and 5% glycerol, 2 mM arginine added, +; 200 μM BH_4 added, +; without BH_4, –.

[a] Relative amplitude, $A_1 + A_2 + A_3 + A_4 = 1$, not including the amplitude of the transient due to the excited state.

The geminate recombination of NO in BA-HNS is slightly affected by the increase of temperature (Fig. 4A). Fig. 4B shows that the extent of recombination in SA-HNS decreases as the temperature is raised from 10 to 30 °C, evidenced by the increase of the asymptotic value A_3, with a concomitant decrease of the amplitude of the nanosecond phase. Because this phase is ill-defined at high temperatures and τ_3 is (2.7 ± 0.4) ns at 20 °C, the data were fitted with two exponential terms and a constant (see Appendix A). The rate of rebinding τ_2 does not vary much, in contrast with the changes in the amplitudes A_2 and A_3 as a function of temperature. Therefore path B rather than path A is adequate. The data have been analyzed according to the general Scheme 1, which shows four states: the NO-liganded heme (H), the unliganded heme (N), an intermediate state or second site (S), and the solution (O). The first (picosecond) component of NO rebinding to both SA and BA-HNS is independent of the temperature and accounts for 50% and 30% of the recombination, respectively. This may represent an intrinsic channel of recombination at short distances ($d \leqslant 3$–4 Å) from the heme iron. Thus, NO rebinding from short distances to the heme is activationless [26,29].

In addition, the rebinding of NO from larger distances, represented by the hundreds of ps to ns process, is regulated by the temperature [28,29,35]. The temperature increase affects the second lifetime τ_2 that decreases while the amplitudes A_2 and A_3 vary in opposite ways. According to model 1, the limiting barrier for NO diffusion is between S and O; the corresponding enthalpy of activation $\Delta H^{\#} = (3.5 \pm 0.7)$

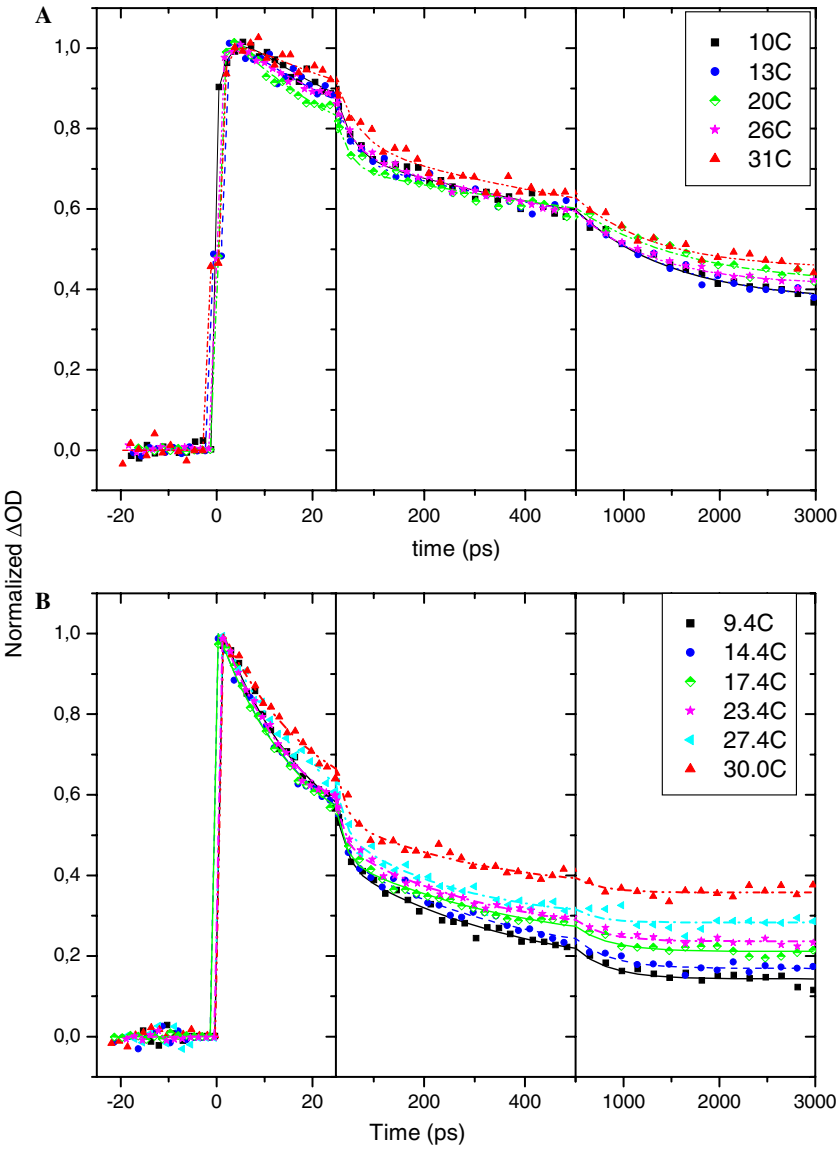

Fig. 4. Effect of temperature on the NO recombination in reduced BA (A) and SA (B) HNS. Proteins (60–100 μM) were reduced by adding dithionite in the presence of 2 mM arginine. The gas phase was equilibrated with 0.1% NO. In the case of BA, each trace represents the mean of two experiments, the first while heating, the second while cooling.

and $(7.9 \pm 0.8)\,\mathrm{kcal\,mol^{-1}}$ for BA-HNS and SA-HNS, respectively, have been calculated. According to the second model, the limiting barrier for recombination is the process leading from S to N, with a minor barrier between S and O. Lower barriers are found in this case: $\Delta H^{\#} = (2.1 \pm 0.4)$ and $(2.9 \pm 0.6)\,\mathrm{kcal\,mol^{-1}}$ for BA-HNS and SA-HNS, respectively.

Effect of the NO concentration on NO geminate rebinding to the ferrous enzymes as a probe of NO dynamics in protein

NO "traffic" within these proteins can be tested by varying the NO concentration. If NO diffusion is "free," then any ligand bound to the protein within roughly 10 Å to the heme can contribute to the recombination. Conversely, the existence of energy barrier(s) and/or any "crowding" effects hindering NO diffusion back to the heme will cancel any contribution from NO ligands at a distance from the heme. These two cases can be distinguished by studying the effect of the NO concentration on the geminate rebinding to the heme.

Effect of the NO concentration on the geminate rebinding in reduced HNS-BA and -SA

Fig. 5A presents the geminate recombination of NO in the reduced BA-HNS. The effect of the NO concentration has been tested within the range 0.02–1%, corresponding to 15–90% saturation, respectively. Thus, the larger noise at the lowest NO concentration originates from the five times smaller signal monitored at 0.02% relative to that measured at 0.1% NO. The normalized decay at [NO] = 0.02% is best fitted by two exponential terms and

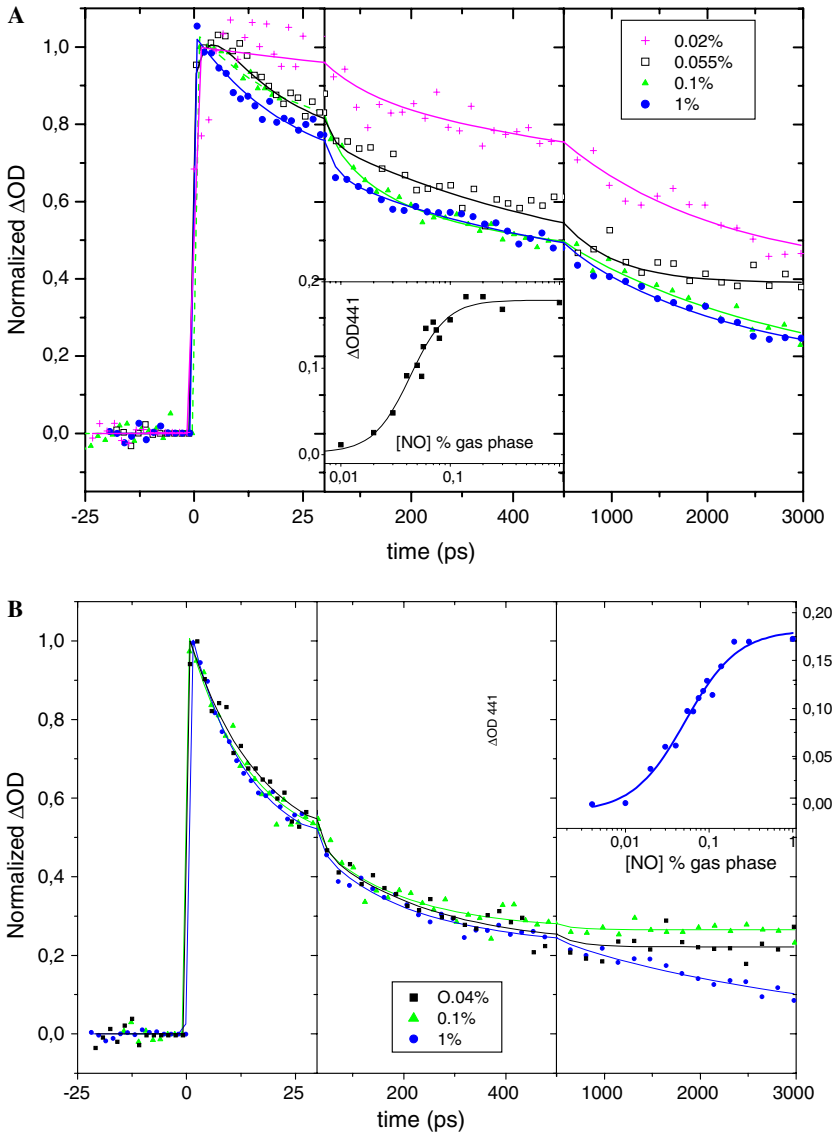

Fig. 5. Effect of the NO concentration on the geminate recombination in the reduced heme of the bacterial proteins. HNS-BA (A), [NO] = 0.02, 0.055, 0.1, 1%: +, □, ▲, ●, respectively; HNS-SA (B), [NO] = 0.04, 0.1 and 1%, ■, ▲, ●, respectively. The insets show an isothermal titration of the reduced proteins with NO; the data are plotted as the difference absorption at a given [NO] with respects to the initial reduced unliganded OD441. The NO concentration is that of the gas phase above the sample. The total pressure is kept constant at 1.3 bars. [protein] = (70–100) μM, same conditions as in Fig. 1. NO concentrations in the gas phase corresponding to half saturation are 0.055, 0.052, and 0.043% for $eNOS_{HD}$, SA-HNS, and BA-HNS, respectively, and point out at a similar affinity of the three proteins for NO.

an asymptotic value. At the concentration of [NO] = 0.055%, the decay becomes faster compared to that observed at [NO] = 0.02%. The first exponential term is shortened from (102 ± 15) ps to (20 ± 3) ps. The constant term decreases from 0.4 to 0.33 and 0.13 with the increase of NO from 0.02 to 0.055 and 0.1%. From [NO] = 0.1% (close to full saturation) to [NO] = 1%, the decays are similar, and are best fitted with three exponentials and a constant (Table 2).

Fig. 5B shows the normalized kinetics of NO rebinding in the reduced SA-HNS at [NO] = 0.04%, 0.1%, and 1%, corresponding to 35%, 75%, and 100% saturation, respectively. The decays are very similar up to 500 ps. There is a small difference on the nanoseconds timescale between the rebinding measured at the different NO concentrations. Given this small difference, our data do not show a significant effect of [NO] on the geminate recombination in the concentration range (0.04–1)%.

Effect of the NO concentration on the geminate recombination in reduced $eNOS_{HD}$

Fig. 6A shows that NO rebinding to $eNOS_{HD}$ is slower at 0.1% NO than at 1% NO. The main effect takes place within picoseconds, where the amplitude of the first exponential term increases from $A_1 = 0.11$ to $A_1 = 0.45$ at 0.1 and 1% NO, respectively (Table 2). The lack of the BH_4 cofactor inhibits the effect of NO concentration on NO rebinding in $eNOS_{HD}$ in the presence of substrate

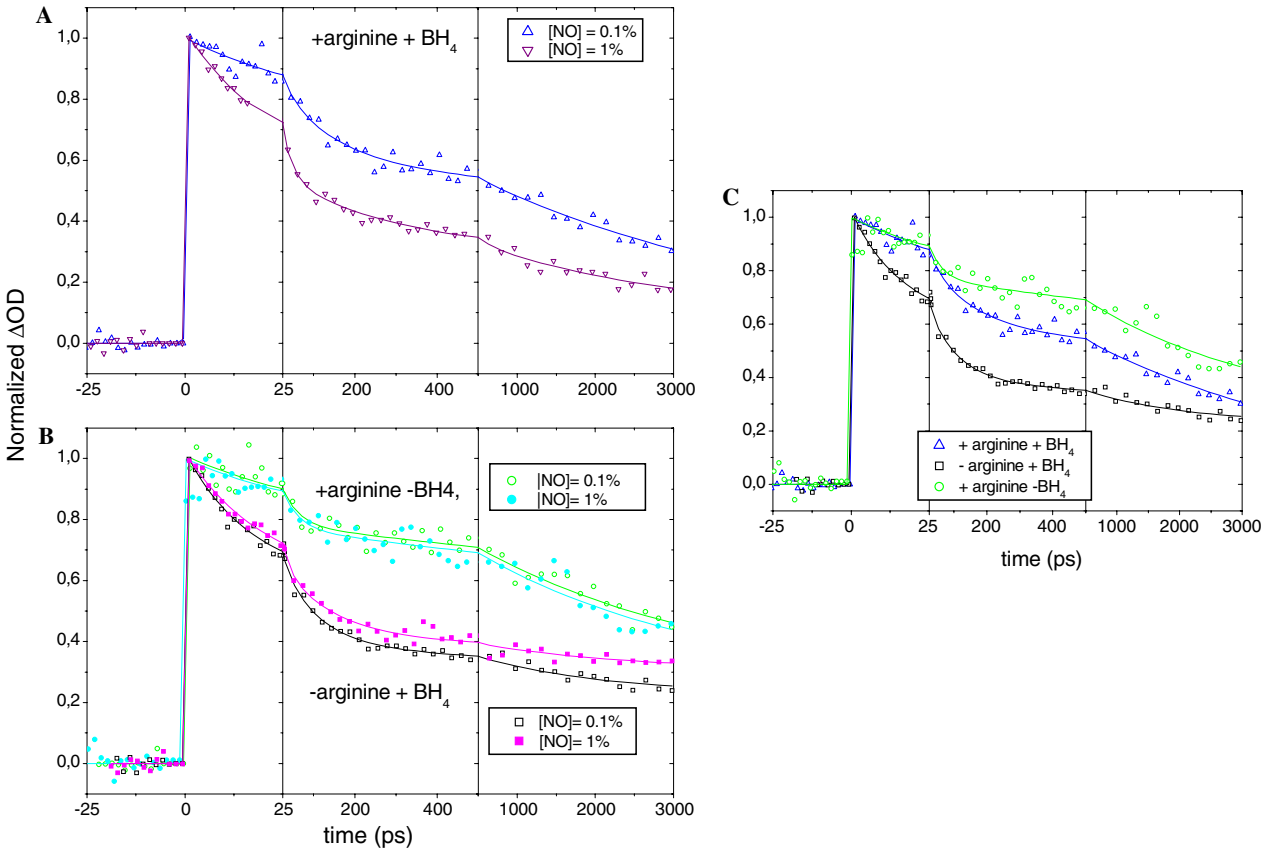

Fig. 6. Geminate recombination of NO in the ferrous $eNOS_{HD}$. (A) Rebinding as a function of the [NO] in the presence of arginine and BH_4, [NO] = 0.1% (▲) and 1% (▽); (B) NO recombination as a function of [NO] in the presence of BH_4 without arginine, upper curves using [NO] = 0.1% (○) or 1% (●); or arginine without BH_4 at 0.1% (□) and 1% NO (■); (C) effect of arginine and BH_4 binding on the geminate recombination at [NO] = 0.1% , +arginine + BH_4, △; −arginine + BH_4, □; +arginine − BH_4, ○.

(Fig. 6B). The same holds true when arginine is lacking in the presence of cofactor (Fig. 6B).

The kinetics data of Fig. 6C indicate that BH_4 lowers the energy barrier for recombination whereas arginine raises it. This is clearly seen in Fig. 6C, from the higher probability of NO escape in the absence of BH_4 and the lower in the absence of arginine.

Discussion

Existence of a second NO site in $eNOS_{HD}$

We previously reported an effect of the NO concentration on the rebinding rate of NO to the heme in the reduced full length eNOS. We attributed this effect to a second NO site within the oxygenase domain. NO diffusion from a secondary site within eNOS could contribute to NO rebinding to the heme, and "gate" the NO traffic from the protein to the solvent and vice versa [23]. Our present data confirm this hypothesis [23]. Migration of the photolyzed ligand to secondary docking sites alternatively interpreted as multiple geminate substates separated by variable inner barriers have been proposed in myoglobin [26–28,35–37]. These sites have been highlighted by X-ray crystallography and time-resolved Laue techniques as they weakly bind xenon [27]. Such cavities have been detected in heme oxygenase [38], nitrophorin 4 [39], cytochromes P450 [40] besides those well-studied of myoglobin [27,37,40]. These cavities often bring flexibility and may define an internal pathway for the migration of a ligand to and from the active site, with a control of function [27]. Ligand migration within the protein matrix to active site involves a limiting number of pre-existing cavities identified in the interior space of the myoglobin [41]. Kinetic evidence for these cavities has been given for cytochrome P450cam, but the docking cavities seem to be either temporary or to have limited access in these enzymes while connected to the access channel to the active site in other cytochrome P450 [28,40]. Direct structural proof of this site is still lacking in eNOS. Although a single structure of NO-bound eNOS (IFOO) was solved by Raman and coworkers at 2 Å resolution [42], identification of a second NO site must wait for a structure solved at a resolution higher than 1.5 Å. Only then, one can distinguish between nitric oxide and a water molecule in an electron density map.

Figs. 6B and C clearly shows that the effect of the NO concentration is only observed with arginine and BH_4. The presence of both the substrate and cofactor is a strict requirement for the accessibility/ viability of the second site. Arginine is seen to increase the probability of NO escape

from eNOS in contrast to BH_4, which limits this escape. Thus, substrate and cofactor have opposite effects on the energy barriers regulating NO release from eNOS. In this way, the second site in eNOS is adapted to the enzyme specific activity and resembles the mechanism of ligand passage along different access channels, apparently adapted to the substrate specificity of each cytochrome P450 [40].

In an attempt to link the kinetics to structure, we first consider the possible electronic coupling of this second site to BH_4 and indirectly to the heme, mediated by hydrogen bonds [7]. Crystallographic data clearly show that both the substrate and the cofactor participate in extensive H-bonding [7,20,21,42–45]. The substrate is held in place by a number of hydrogen bonds, both at the level of the guanidinium moiety by the conserved Glu363 [46] and NO and at the other extremity by Tyr359 and Asn368 in eNOS (1FOP [42], Scheme 1). The phenyl ring of Tyr359 is in close proximity to the heme, Trp358 and BH_4 aromatic ring. Arg252 is also located close (3.5 Å) to the carboxylic extremity of the substrate. In order to decrease the energy barrier, the second site was assumed to be located close to the BH_4 site [23]. This hypothesis is consistent with BH_4 decreasing the heme potential [47]. We show that arginine also regulates NO escape, but in an opposite way to BH_4. In addition, arginine slightly increases the heme potential [48]. The second site, presumably located in the heme pocket, may alternatively be close to arginine and the coupling between the substrate, cofactor and heme is likely to involve indirect interactions, via the extensive H-bonding network between them. The close proximity of Arg252 and Tyr359, Trp358 and BH_4 aromatic ring to the heme makes them likely candidates to take part in the control of NO geminate recombination. Long range action transmitted via loose H-bonds to the substrate and between the latter and NO could finely tune the positioning of the substrate and influence the geminate recombination of NO to the heme in eNOS.

In addition, the effect of arginine and BH_4 on NO rebinding may also arise from conformational fluctuations induced by the substrate and cofactor. eNOS structure and spin state are influenced by the conjugated effects of arginine and BH_4. However, it is thought to rigidify the heme, arguing against structural fluctuations [7,43]. Interestingly, in the related protein P450cam, this relaxation process was found strongly dependent on the substrate with a steep effect of the temperature [28].

Second site identified in BA-HNS but inaccessible or absent in SA-HNS at 20 °C? Effect of temperature to identify energy barriers limiting NO escape in SA-HNS

NO rebinding in BA-HNS (Fig. 5A) clearly presents a similar effect of the NO concentration as shown in eNOS. The opposite holds true for SA-HNS. Thus, a free diffusion of NO ligands between a second (docking) site and the heme occurs in BA-HNS at 20 °C. In contrast, the lack of NO concentration effect may have two alternative explanations: [1] the heme pocket is too small to allow the binding of two NO ligands; in this case, steric effects hinder NO recombination to the heme; [2] this site is not accessible; NO migration from this site is restricted by energy barriers at 20 °C and only dissociated NO in close vicinity rebinds to the heme. The heme pocket of SA-HNS is quite large as for $eNOS_{HD}$, arguing against the first hypothesis of steric hindrance [15]. To test the second hypothesis, we measured NO rebinding to the heme in both HNS as a function of temperature. We analyzed the data according to two models (Scheme 3 and Appendix A). In both models, there is a first recombination process taking place within the 20 ps range that is found independent of the temperature. Thus, the fast rebinding from N to H is activationless, as it also occurs in MbNO [29]. The slower phase is found dependent on the temperature and was analyzed according to two models. In the first model, a larger energy barrier of $\Delta H^{\#} = (7.9 \pm 0.8)\,\mathrm{kcal\,mol^{-1}}$ separates between S and O in SA-HNS compared to $\Delta H^{\#} = (3.5 \pm 0.7)$ in BA-HNS. According to the second model, the limiting barrier for recombination is the process leading from S to N, with a minor barrier between S and O. Lower barriers are found in this case: $\Delta H^{\#} = (2.1 \pm 0.4)$ and $(2.9 \pm 0.6)\,\mathrm{kcal\,mol^{-1}}$ for BA-HNS and SA-HNS, respectively. These last set of values are closer to that found for the slow geminate phase of ~200 ps in MbNO: $\Delta H = 3\,\mathrm{kJ\,mol^{-1}}$ ($0.72\,\mathrm{kcal\,mol^{-1}}$) [29]. The much larger heme pockets of eNOS and SA-HNS as compared to myoglobin likely require larger migration of NO from a second site or cavity to the heme, in agreement with slower rebinding rates, associated with larger activation energies. Mutations showed that the size of the distal pocket was indeed a major determinant governing the rate of ligand entry into myoglobin [37].

It should be emphasized that the above analysis assumes that the kinetic variation results from temperature-induced difference of NO migration rate within the proteins, provided the protein structure remains unchanged in the range 5–33 °C. All NOS structures were solved at 100 K and no direct proof of the validity of the above assumption exists. Nevertheless, X-ray structures of other model proteins such as myoglobin, lysozyme or RNase A solved between 80 and 300 K are very similar in this temperature range [41,49–51]. These observations suggest that between 278 and 306 K, the protein structures of $eNOS_{HD}$, BA-, and SA-HNS should not show any major changes that could affect the dynamic of NO rebinding.

Links between kinetics and structure

Role of the substrate in the three oxidized proteins

Fig. 2A shows that NO rebinding to the heme in SA-HNS and BA-HNS present very similar kinetics, especially in the first 50 ps when arginine is absent. This suggests modifications in the immediate vicinity to the heme when the arginine substrate is absent. In these conditions, the D ring propionate (propD) is H-bonded to BH_4 in eNOS, but not

in BA and SA-HNS (Schemes 1 and 3). Since, in our hands, BH_4 is not binding to both BA and SA-HNS, the propD will be fully accessible to solvent. This should alter the heme potential and may explain why NO rebinding is enhanced and similar in BA- and SA-HNS in absence of arginine. In addition, the comparison of eNOS and SA-HNS structures point out that the dimer is more open by 5.3 degrees offset between the two monomers in SA-HNS than in eNOS [15,43]. Therefore, the conserved residues Y359, W332, Y333, R252, and Q249 are slightly shifted from the substrate site, modifying their H-bonding interactions with NO and the heme. This may contribute to variations of the energy barriers for NO rebinding and explain why BA and SA are clustered in the absence of arginine and differs from $eNOS_{HD}$.

The similarity between the two HNS no longer holds in the presence of arginine (Fig. 2B). These data suggest that the arginine H-bonding interactions and/or its dynamics differ in the two bacterial proteins and affect NO recombination in the oxidized HNS. The instability of the reduced nitrosyl complexes does not allow such a comparison for the reduced HNS in the absence of arginine (data not shown). The large effect of arginine at short timescales (ps) is consistent with a change in the geometry of the ferric heme induced by the substrate binding. Resonance Raman studies point out at low-frequency, pyrole vibrational modes observed on addition of arginine to eNOS [52]. These modes were attributed to change in heme geometry, possibly coupled hydrogen bonding to the thiolate and to an increase of the redox potential resulting

```
        130         140         150         160         170         180
1   LSQARDFINQYYSSIKRSGSQAHEERLQEVEAEVASTGTYHLRESELVFGAKQAWRNAPR  184 eNOS
2   FPLAKEFIDQYYSSIKRFGSKAHMERLEEVNKEIDTTSTYQLKDTELIYGAKHAWRNASR  419 nNOS
3   LPQAIEFVNQYYGSFKEAKIEEHLARVEAVTKEIETTGTYQLTGDELIFATKQAWRNAPR  126 iNOS
4   FKEAQAFIENMYKECHY-ETQIINKRLHDIELEIKETGTYTHTEEELIYGAKMAWRNSNR   61 HNSSA
5   IEEASHFITICYKELS--KEHFIEERMKEIQAEIEKTGTYEHTFEELVHGSRMAWRNSNR   65 HNSBA
C   :::A.:F*:++Y:+:+:.::::+:+R+:++::E*::T*TY:++::EL+:*+*:AWRN+:R

        190         200         210         220         230         240
1   CVGRIQWGKLQVFDARDCSSAQEMFTYICNHIKYATNRGNLRSAITVFPQRAPGRGDFRI  244 eNOS
2   CVGRIQWSKLQVFDARDCTTAHGMFNYICNHVKYATNKGNLRSAITIFPQRTDGKHDFRV  479 nNOS
3   CIGRIQWSNLQVFDARSCSTAREMFEHICRHVRYSTNNGNIRSAITVFPQRSDGKHDFRV  186 iNOS
4   CIGRLFWDSLNVIDARDVTDEASFLSSITYHITQATNEGKLKPYITIYAPKDGP----KI  117 HNSSA
5   CIGRLFWSKMHILDAREVNDEEGVYHALIHHIKYATNDGKVKPTITIFKQYQGEENNIRI  125  HNSBA
C   C+GR++W+++*+*+DAR++::+.:++.:*+:H++**TN.G+++++IT+*+*+.:+::++*+

        250         260         270         280         290         300
1   WNSQLVRYAGYRQQDGSVRGDPANVEITELCIQHGWTPGNGRFDVLPLLLQAPDEAPELF  304 eNOS
2   WNSQLIRYAGYKQPDGSTLGDPANVQFTEICIQQGWKPPRGRFDVLPLLLQANGNDPELF  539 nNOS
3   WNAQLIRYAGYQMPDGSIRGDPANVEFTQLCIDLGWKPKYGRFDVVPLVLQANGRDPELF  246 iNOS
4   FNNQLIRYAGYDNCG-----DPAEKEVTRLANHLGWKGKGTNFDVLPLIYQLPNESVKFY  172 HNSSA
5   YNHQLIRYAGYKTEMG-VTGDSHSTAFTDFCQELGWQGEGTNFDVLPLVFSIDGKAPIYK  184 HNSBA
C   +N:QL*RYAGY:::+*+::*D**++++T:+*+:+GW++:::++FDV*PL:+*+:+::*+++

        310         320         330         340         350         360
1   VLPPELVLEVPLEHPTLEWFAALGLRWYALPAVSNMLLEIGGLEFSAAPFSGWYMSTEIG  364 eNOS
2   QIPPELVLEVPIRHPKFEWFKDLGLKWYGLPAVSNMLLEIGGLEFSACPFSGWYMGTEIG  599 nNOS
3   EIPPDLVLEVAMEHPKYEWFRELELKWYALPAVANMLLEVGGLEFPGCPFNGWYMGTEIG  306 iNOS
4   EYPTSLIKEVPIEHNHYPKLRKLNLKWYAVPIISNMDLKIGGIVYPTAPFNGWYMVTEIG  232 HNSSA
5   EIPKEEVKEVPIEHPEYP-ISSLGAKWYGVPMISDMRLEIGGISYTAAPFNGWYMGTEIG  243 HNSBA
C   ++P++**+EV*+*H*:++++:.L+**WY++P+++**M+L**GG+++:++PF+GWYM+TEIG

        370         380         390         400         410         420
1   TRNLCDPHRYNILEDVAVCMDLDTRTTSSLWKDKAAVEINLAVLHSFQLAKVTIVDHHAA  424 eNOS
2   VRDYCDNSRYNILEEVAKKMNLDMRKTSSLWKDQALVEINIAVLYSFQSDKVTIVDHHSA  659 nNOS
3   VRDFCDVQRYNILEEVGRRMGLETHKLASLWKDQAVVEINIAVLHSFQKQNVTIMDHHSA  366 iNOS
4   VRNFIDDYRYNLLEKVADAFEFDTLKNNSFNKDRALVELNYAVYHSFKKEGVSIVDHLTA  292 HNSSA
5   ARNLADHDRYNLLPAVAEMMDLDTSRNGTLWKDKALIELNVAVLHSFKKQGVSIVDHHTA  303 BANOS
C   +R+:+D..RYN+L*:V*..*:***:+::***KD:A+*E+N:AV**SF++::V+I*DH*:A

        430         440         450         460         470         480
1   TVSFMKHLDNEQKARGGCPADWAWIVPPISGSLTPVFHQEMVNYILSPAFRYQPDPWKGS  484 eNOS
2   TESFIKHMENEYRCRGGCPADWVWIVPPMSGSITPVFHQEMLNYRLTPSFEYQPDPWNTH  719 nNOS
3   AESFMKYMQNEYRSRGGCPADWIWLVPPMSGSITPVFHQEMLNYVLSPFYYYQVEAWKTH  426 iNOS
4   AKQFELFERNEAQQGRQVTGKWSWLAPPLSPTLTSNYHHGYDNTVKDPNFFYKKKESNAN  352 HNSSA
5   AQQFQQFEKQEAACGRVVTGNWVWLIPPLSPATTHIYHKPYPNEILKPNFFHK-------  356 HNSBA
C   +:+F:+:::.*E:::+++++++W:W++PP:S++:T+++H+++:N+:*:P:*:*+:::+:::
```

Scheme 2. Multiple Alignment. The sequences of 1: iNOS (1NSI), 2: nNOS (1OM4), 3: eNOS (1FOP), 4: SA NOS (1MJT), 5: BA NOS have been aligned using the Edtaln sofware (Infobiogen, Pasteur Institute). The consensus C are the following: "." The AA has a représentation $\geqslant$20%, ":" $\geqslant$40%, "+" $\geqslant$60%, "*" $\geqslant$80%, the AA itself, when identical in all sequences. The bold red letters correspond to residues involved in L-arginine or cofactor binding; the grey areas correspond to the sequences involved in H-bonding with propionate C (in eNOS), as mentioned in the text. R252 (eNOS) is shown in green; it is mentioned in the text as a residue likely involved in the control of NO release. (For interpretation of the references to color in this figure legend, the reader is referred to the web version of this paper.)

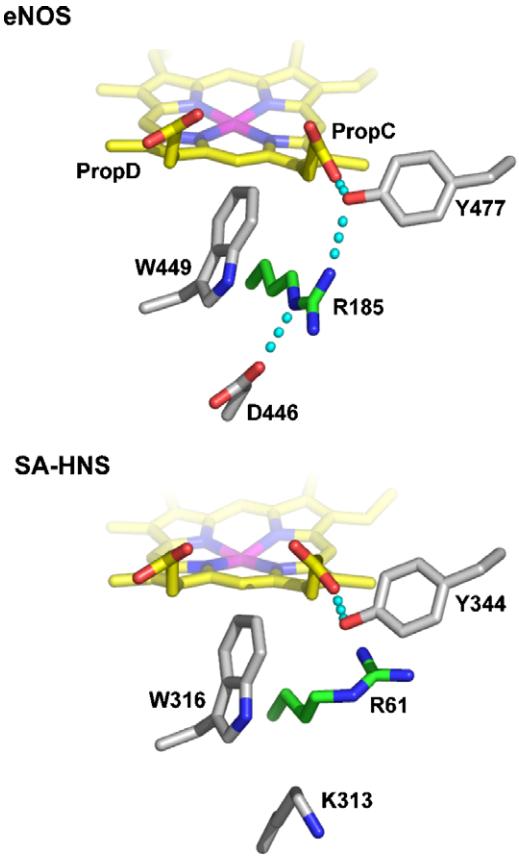

Scheme 3. Close-up to the H-bonding networks in eNOS compared to that in SA-HNS that could regulate differently the energy barrier(s) for NO rebinding in the studied proteins. Upper part: eNOS [42]: Ring C propionate (yellow) is H-bonded to Y477 (grey) and R185 (green); the latter is held in place by an H-bond to D446. Oxygen and nitrogen atoms are represented in red and blue, respectively. Lower part: SA-HNS [15]: Ring C propionate is only H-bonded to Y344; note the position of R61 away from K313. (For interpretation of the references to color in this figure legend, the reader is referred to the web version of this paper.)

from a non-planarity of the heme [52]. Differential electronic coupling effects may also modify the distance between the guanidium moiety of the substrate and the heme, allowing or preventing H-bonding between arginine and NO. Our data support a dynamic effect of arginine that could be consistent with the substrate binding flexibility.

Hypothesis on the residues responsible for the differences in NO rebinding rates

(i) Sequence alignment (Scheme 2) showed that a conserved valine in mammalian NOS was changed into isoleucine in HNS proteins. Mutation of this conserved Val into Ile in the inducible $iNOS_{HD}$ decreased by 10-fold the dissociation constant of NO from the ferric enzyme [17]. This valine to isoleucine mutation was shown to induce steric effects between the Ile methyl group and the heme-bound NO in *B. subtilis* [17]. Thus, if this mutation was the main factor controlling NO recombination to the heme, one would expect a similar rebinding rate in BA and SA-HNS, faster than that in $eNOS_{HD}$. Figs. 2 and 3 clearly point out differences in recombination rates between the bacterial enzymes BA-HNS and SA-HNS enzymes in the presence of arginine, both proteins having an Ile. Replacing the arginine substrate by *N*-hydroxyarginine resulted in slower NO rebinding kinetics in both BA-HNS and $eNOS_{HD}$ (data not shown). It is only in the absence of arginine that we observe similar rates of NO geminate recombination and very low probabilities of NO escape ($A_4 = 0.05$–0.09) in both bacterial enzymes. In these conditions, NO rebinding in HNS is faster than that observed with $eNOS_{HD}$ (Fig. 2A). Our data thus do not support the hypothesis of the switch of Val to Ile as a major determinant controlling NO release in conditions where the substrate is present. However, caution should be taken when comparing proteins that differ from more than one point mutation; other variable residues in close proximity could contribute as well, as for example Asn340 (eNOS), conserved in the mammalian NOS and SA-HNS is replaced by Asp a charged residue in BA-HNS (as well as in *B. subtilis* and *Deinococcus*). Thus, the effect of valine to isoleucine on NO release could also be tested by measuring NO rebinding rates due to point mutations within the same protein.

(ii) In order to identify variable residues among the various NOS and HNS enzymes that could contribute to changes in NO rebinding, a selection according to their distance from the heme iron was applied. We used the rough cut-off distance of residues located within 7–10 Å from the iron, consistent with NO migration distances in the timescales of our measurements. We found that an H-bonding network in eNOS links ring C propionate (propC) to R185 via Y477; R185 also forms an H-bond with D446 (Scheme 3). In BA-HNS, the propionate C could still be H-bonded to R65 and N324, despite the change of Y477 (eNOS) into H355 (BA-HNS). In SA-HNS, the hydrogen bonding between the propionate C and R61 is lost; the latter is also unable to form an H-bond with K313 (as compared to D446 in eNOS). Thus, SA-HNS propC can only be H-bonded to Y344. We therefore suggest that R185 may play a key role by hydrogen bonding or not to the ring C propionate. This H-bonding is likely to modulate the energy barriers for NO recombination and modify the heme redox potential. In eNOS and most likely in BA-HNS, the hydrogen bonding network between the propC and R185 might result in a similar NO rebinding in the presence of the arginine substrate, in contrast with SA-HNS for which this H-bond is nonexistent. R185 is further modulated by D446. This latter residue, although located 13 Å from the iron may introduce different electrostatic effects, especially in SA-HNS where it becomes a lysine compared to N324 in BA-HNS.

Our work provides a structural dynamic perspective on the bacterial HNS proteins compared to the endothelial $eNOS_{HD}$. It proposes testable hypotheses with respect to residues involved in the regulation of NO release from these proteins. Work in this direction is in progress.

Acknowledgment

Structure–function work on bacterial NOS-like proteins in the Raman laboratory is funded by: the NIH (R01 AI054444), the Pew Charitable Trusts via a Pew Scholar Award, and The Robert A. Welch Foundation (AU-1524). P.N. was a postdoctoral fellow of the Association pour la Recherche sur le Cancer (ARC). I.M. and P.M. are supported by grants MSMT of Czech Republic No. 0021620806 and GAUK 21/C/2004; Dr M.H. Vos is acknowledged for helpful discussions. C.S.R. is grateful to the Cold Spring Harbor Laboratory's course (June 2000) on "Molecular Cloning of Neural Genes" for providing him with laboratory facilities and reagents to clone SA- and BA-HNS.

Appendix A

Each exponential term τ_1 and τ_2, used to fit the experimental rebinding curves shown in Fig. 4 (listed in the below table), are a sum of the forward and backward process, $1/\tau_1 = k1 + k\text{-}2$ and $1/\tau_2 = k2 + k\text{-}3$, where $k1$ is the rate of NO rebinding from N to H, $k2$ from S to N, k-2 from N to S and k-3 from S to O. The amplitude terms gives the ratios of rate constants.

T (°C)	τ1 (ps)	$A1$	τ2 (ps)	$A2$	$A3$
SA-HNS	±2		±35		
9.4	18.1	0.566	353	0.297	0.137
14.4	16.9	0.537	357	0.296	0.167
17.4	16.9	0.546	359	0.246	0.208
23.5	15.7	0.522	310	0.252	0.227
27.5	17.5	0.489	243	0.238	0.273
30	18.2	0.462	286	0.194	0.344
BA-HNS	±5		±90		
9.4	30.9	0.310	997	0.350	0.340
11.6	30.2	0.350	1168	0.295	0.355
14.4	30.9	0.270	997	0.398	0.332
19.4	24.9	0.351	1203	0.258	0.391
20	23.1	0.340	1070	0.285	0.375
25.4	35.3	0.250	832	0.310	0.440
27.4	28.8	0.313	778	0.342	0.345
29.0	38.4	0.220	863	0.274	0.506

In the first model, it is assumed that there is no contribution of ligands from the solution to NO rebinding, meaning that $k3$ (from 0 to S) is much slower than the other rate constants; the second model assumes that there could be some contribution from the bulk. The details are given in the below table (model 1and 2: left and right entries, respectively; lines 2–7: SA-HNS; lines 9–16: BA-HNS).

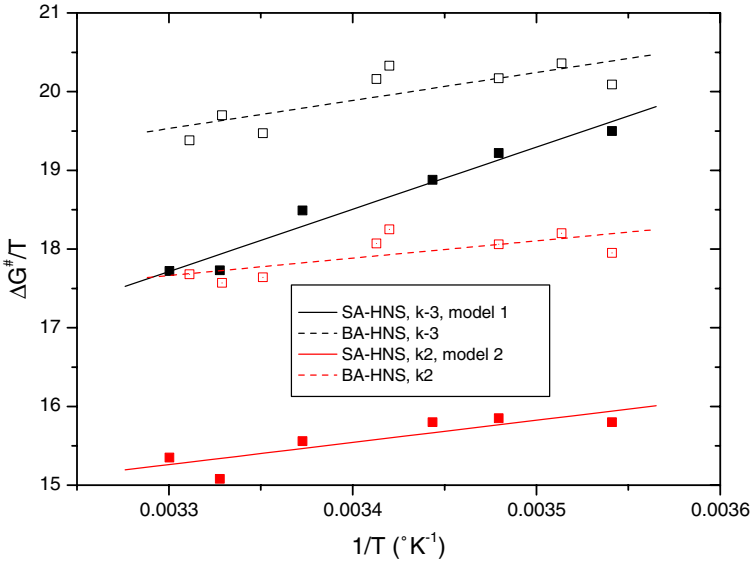

$1/T$ (K^{-1})	$k1$ (s^{-1})	k-2 (s^{-1})	$k2$ (s^{-1})	k-3 (s^{-1})	$k1$(s^{-1})	k-2 (s^{-1})	$k2$ (s^{-1})	k-3 (s^{-1})
3.541E−03	4.261E+10	1.264E+10	2.488E+09	3.420E+08	3.528E+10	1.996E+10	2.182E+09	6.474E+08
3.479E−03	4.566E+10	1.352E+10	2.401E+09	4.002E+08	3.849E+10	2.068E+10	2.161E+09	6.398E+08
3.444E−03	4.748E+10	1.169E+10	2.308E+09	4.808E+08	3.829E+10	2.089E+10	2.238E+09	5.508E+08
3.373E−03	5.089E+10	1.281E+10	2.626E+09	5.953E+08	4.186E+10	2.184E+10	2.574E+09	6.477E+08

(*continued on next page*)

Appendix A (*continued*)

$1/T$ (K^{-1})	$k1$ (s^{-1})	k-2 (s^{-1})	$k2$ (s^{-1})	k-3 (s^{-1})	$k1$(s^{-1})	k-2 (s^{-1})	$k2$ (s^{-1})	k-3 (s^{-1})
3.328E−03	4.616E+10	1.099E+10	3.237E+09	8.831E+08	3.837E+10	1.877E+10	3.328E+09	7.923E+08
3.300E−03	4.601E+10	8.935E+09	2.605E+09	8.964E+08	3.759E+10	1.735E+10	2.932E+09	5.694E+08
3.541E−03	2.397E+10	8.390E+09	7.485E+08	2.545E+08	2.470E+10	7.658E+09	7.430E+08	2.600E+08
3.514E−03	2.557E+10	7.543E+09	6.319E+08	2.243E+08	2.453E+10	8.585E+09	6.611E+08	1.950E+08
3.479E−03	2.314E+10	9.218E+09	7.533E+08	2.497E+08	2.548E+10	6.884E+09	7.173E+08	2.857E+08
3.420E−03	3.193E+10	8.229E+09	5.974E+08	2.339E+08	2.973E+10	1.043E+10	6.609E+08	1.703E+08
3.413E−03	3.369E+10	9.601E+09	6.799E+08	2.550E+08	3.231E+10	1.098E+10	7.276E+08	2.074E+08
3.351E−03	2.162E+10	6.704E+09	8.343E+08	3.671E+08	2.266E+10	5.666E+09	9.171E+08	2.843E+08
3.329E−03	2.587E+10	8.854E+09	9.555E+08	3.298E+08	2.645E+10	8.269E+09	9.576E+08	3.277E+08
3.311E−03	2.044E+10	5.601E+09	7.695E+08	3.894E+08	2.135E+10	4.696E+09	9.096E+08	2.492E+08

References

[1] L.J. Ignarro, in: L. Ignarro (Ed.), Nitric Oxide Biology and Pathobiology, Academic Press, San Diego, CA, 2000.

[2] D. Wendehenne, A. Pugin, D.F. Klessig, J. Durner, Nitric oxide: comparative synthesis and signaling in animal and plant cells, Trends Plant Sci. 6 (4) (2001) 177–183.

[3] Vollack, Zumft, Nitric oxide signaling and transcriptional control of denitrification genes in *Pseudomonas stutzeri*, J. Bact. 183 (2001) 2516.

[4] H. Corker, R.K. Poole, Nitric oxide formation by *Escherichia coli*. Dependence on nitrite reductase, the NO-sensing regulator Fnr, and flavohemoglobin Hmp, J. Biol. Chem. 278 (2003) 31584.

[5] W.G. Zumft, Cell biology and molecular basis of denitrification, Microbiol. Mol. Biol. Rev. 61 (4) (1997) 533–616.

[6] D.S. Bredt, P.M. Hwang, C.E. Glatt, C. Lowenstein, R.R. Reed, S.H. Snyder, Cloned and expressed nitric oxide synthase structurally resembles cytochrome P-450 reductase, Nature 351 (1991) 714–718.

[7] C.S. Raman, P. Martasek, B.S.S. Masters, in: The Porphyrin Handbook, K.M. Kadish, K. M. Smith, R. Guilard (Eds.), vol. 4, 2000, pp. 293–339.

[8] Y. Chen, J.P.N. Rosazza, Purification and characterization of nitric oxide synthase (NOSNoc) from a Nocardia species, J. Bacteriol. Sept 5 (1995) 122–128.

[9] H. Morita, H. Yoshikawa, R. Sakata, Y. Nagata, H. Tanaka, Synthesis of nitric oxide from the two equivalent guanidino nitrogens of L-arginine by Lactobacillus fermentum, J. Bacteriol. 179 (1997) 7812–7815.

[10] W.S. Choi, M.S. Chang, J.W. Han, S.Y. Hong, H.W. Lee, Identification of nitric oxide synthase in *Staphylococcus aureus*, Biochem. Biophys. Res. Commun. 237 (3) (1997) 554–558.

[11] K. Pant, A.M. Bilwes, S. Adak, D.J. Stuehr, B.R. Crane, Structure of a nitric oxide synthase heme protein from *Bacillus subtilis*, Biochemistry 41 (37) (2002) 11071–11079.

[12] S. Adak, K.S. Aulak, D.J. Stuehr, Direct evidence for nitric oxide production by a nitric-oxide synthase-like protein from *Bacillus subtilis*, J. Biol. Chem. 27 (18) (2002) 16167–16171.

[13] K. Pant, B.R. Crane, Structure of a loose dimer in nitric oxide synthase assembly, J. Mol. Biol. 352 (2005) 932–940.

[14] S. Adak, A.M. Bilwes, K. Panda, D. Hosfield, K.S. Aulak, J.F. McDonald, J.A. Tainer, E.D. Getzoff, B.R. Crane, D.J. Stuehr, Cloning, expression, and characterization of a nitric oxide synthase protein from *Deinococcus radiodurans*, Proc. Natl. Acad. Sci. USA 99 (1) (2002) 107–112.

[15] L.E. Bird, J. Ren, J. Zhang, N. Foxwell, A.R. Hawkins, I.G. Charles, D.K. Stammers, Crystal structure of SANOS, a bacterial nitric oxide synthase oxygenase protein from *Staphylococcus aureus*, Structure (Camb). 10 (12) (2002) 1687–1696.

[16] M.R. Buddha, B.R. Crane, Structure and activity of an aminoacyl-tRNA synthetase that charges tRNA with nitro-tryptophan, Nat. Struct. Mol. Biol. 12 (3) (2005) 274–275.

[17] Z.Q. Wang, C.C. Wei, M. Sharma, K. Pant, B.R. Crane, D.J. Stuehr, A conserved Val to Ile switch near the heme pocket of animal and bacterial nitric-oxide synthases helps determine their distinct catalytic profiles, J. Biol. Chem. 279 (18) (2004) 19018–19025.

[18] J.A. Kers, M.J. Wach, S.B. Krasnoff, J. Widom, K.D. Cameron, R.A. Bukhalid, D.M. Gibson, B.R. Crane, R. Loria, Nitration of a peptide phytotoxin by bacterial nitric oxide synthase, Nature 429 (2004) 79–82.

[19] M.R. Buddha, T. Tao, R.J. Parry, B.R. Crane, An unusual tryptophanyl tRNA synthetase interacts with nitric oxide synthase in *Deinococcus radiodurans*, J. Biol. Chem. 279 (2004) 49567–49570.

[20] P. Martasek, P. Nioche, A.-L. Tsai, C.S. Raman, in: 12th International Conference on Cytochrome P450, La Grande Motte, France, Abstract, 2001, P606.

[21] C.S. Raman, ibid., CL2-3, (2001).

[22] M. Negrerie, V. Berka, M.H. Vos, U. Liebl, J.C. Lambry, A.L. Tsai, J.L. Martin, Geminate recombination of nitric oxide to endothelial nitric-oxide synthase and mechanistic implications, J. Biol. Chem. 274 (35) (1999) 24694–24702.

[23] A. Slama-Schwok, M. Négrerie, V. Berka, J.C. Lambry, A.L. Tsai, M.H. Vos, J.L. Martin, Nitric oxide (NO) traffic in endothelial NO synthase. Evidence for a new NO binding site dependent on tetrahydrobiopterin? J. Biol. Chem. 277 (2002) 7581–7586.

[24] J. Santolini, A.L. Meade, D.J. Stuehr, Differences in three kinetic parameters underpin the unique catalytic profiles of nitric-oxide synthases I, II, and III*, J. Biol. Chem. 276 (2001) 48887–48898.

[25] H.M. Abu-Soud, K. Ichimori, A. Presta, D.J. Stuehr, Electron transfer, oxygen binding, and nitric oxide feedback inhibition in endothelial nitric-oxide synthase, J. Biol. Chem. 275 (2000) 17349–17357.

[26] J.-L. Martin, M.H. Vos, Femtosecond biology, Annu. Rev. Biophys. Biomol. Struct. 21 (1992) 199–222.

[27] M. Brunori, D. Bourgeois, B. Vallone, The structural dynamics of myoglobin, J. Struct. Biol. 147 (2004) 223–234.

[28] C. Treteau, D. Lavalette, Dominant features of protein reaction dynamics: conformational relaxation and ligand migration, Biochem. Biophys. Acta 1724 (2005) 411–424.

[29] D. Ionascu, F. Gruia, X. Yu, F. Rosca, C. Beck, A. Demidov, J.S. Olson, P.M. Champion, Temperature-dependent studies of NO recombination to the heme and heme proteins, J. Am. Chem. Soc. 127 (2005) 16921–16934.

[30] J.S. Nishimura, P. Martasek, K. McMillan, J. Salerno, Q. Liu, S.S. Gross, B.S. Masters, Modular structure of neuronal nitric oxide synthase: localization of the arginine binding site and modulation by pterin, Biochem. Biophys. Res. Commun. 210 (1995) 288–294.

[31] G. Eberlein, T.C. Bruice, R.A. Lazarus, R. Henrie, S.J. Benkovic, The interconversion of the 5,6,7,8-tetrahydro-, 6,7,8-dihydro-, and radical forms of 6,6,7,7-tetramethyldihydropterin. A model for the biopterin center of aromatic amino acid mixed function oxidases, J. Am. Chem. Soc. 106 (1984) 7916–7924.

[32] J. Petrich, C. Poyart, J.-L. Martin, Photophysics and reactivity of heme proteins: a femtosecond absorption study of hemoglobin, myoglobin, and protoheme, Biochemistry 27 (1988) 4049–4060.

[33] W.H. Press, S.A. Teukolsky, W.T. Vetterling, B.P. Flannery, Numerical Recipies, Cambridge University Press, Cambridge, UK, 1988.

[34] C.S. Raman, R. Jemmerson, B.T. Nall, M.J. Allen, Diffusion-limited rates for monoclonal antibody binding to cytochrome *c*, Biochemistry 31 (1992) 10370–10379.
[35] D.C. Lamb, K. Nienhaus, A. Arcovito, F. Draghi, A.E. Miele, M. Brunori, G.U. Nienhaus, Structural dynamics of myoglobin: ligand migration among protein cavities studied by Fourier transform infrared/temperature derivative spectroscopy, J. Biol. Chem. 277 (2002) 11636–11644.
[36] S. Kim, G. Jin, M. Lim, Dynamics of geminate recombination of NO with myoglobin in aqueous solution probed by femtosecond mid-IR spectroscopy, J. Phys. Chem. 108 (2004) 20366–20375.
[37] E.E. Scott, Q.H. Gibson, J.S. Olson, Mapping the pathways for O2 entry into and exit from myoglobin, J. Biol. Chem. 276 (2001) 5177–5188.
[38] M. Sugishima, H. Sakamoto, M. Noguchi, K. Fukuyama, CO-trapping site in heme oxygenase revealed by photolysis of its CO-bound heme complex: mechanism of escaping from product inhibition, J. Mol. Biol. 341 (2004) 7–13.
[39] K. Nienhaus, E.M. Maes, A. Weichsel, W.R. Montfort, G.U. Nienhaus, Structural dynamics controls nitric oxide affinity in nitrophorin 4, J. Biol. Chem. 279 (2004) 39401–39407.
[40] R.C. Wade, P.J. Winn, I. Schlichting, Sudarko, A survey of active site access channels in cytochromes P450, J. Inorg. Biochem. 98 (2004) 1175–1182.
[41] M. Brunori, B. Vallone, F. Cutruzzola, C. Travaglini-Allocatelli, J. Berendzen, K. Chu, R.M. Sweet, I. Schlichting, The role of cavities in protein dynamics: crystal structure of a photolytic intermediate of a mutant myoglobin, Proc. Natl. Acad. Sci. USA 97 (2000) 2058–2063.
[42] H. Li, C.S. Raman, P. Martasek, B.S.S. Masters, T.L. Poulos, Crystallographic studies on endothelial nitric oxide synthase complexed with nitric oxide and mechanism-based inhibitors, Biochemistry 40 (2001) 5399.
[43] C.S. Raman, H. Li, P. Martasek, V. Kral, B.S. Masters, T.L. Poulos, Crystal structure of constitutive endothelial nitric oxide synthase: a paradigm for pterin function involving a novel metal center, Cell 95 (7) (1998) 939–950.
[44] T.O. Fischmann, A. Hruza, X.D. Niu, J.D. Fossetta, C.A. Lunn, E. Dolphin, A.J. Prongay, P. Reichert, D.J. Lundell, S.K. Narula, P.C. Weber, Nat. Struct. Biol. 6 (1999) 233–242.
[45] Y. Sato, I. Sagami, T. Matsui, T. Shimizu, Unusual role of Tyr588 of neuronal nitric oxide synthase in controlling substrate specificity and electron transfer, Biochem. Biophys. Res. Commun. 281 (2001) 621–626.
[46] R. Gachhui, D.K. Ghosh, C. Wu, J. Parkinson, B.R. Crane, D.J. Stuehr, Mutagenesis of acidic residues in the oxygenase domain of inducible nitric-oxide synthase identifies a glutamate involved in arginine binding, Biochemistry 36 (1997) 5097–5103.
[47] A. Presta, A.M. Weber-Main, M.T. Stankoich, D.J. Stuehr, Comparative effects of substrates and pterin cofactor on the heme midpoint potential in inducible and neuronal nitric oxide synthase, J. Am. Chem. Soc. 120 (1998) 9460–9465.
[48] Y.T. Gao, S.M.E. Smith, J.B. Weinberg, H.J. Montgomery, E. Newman, J.G. Guillemette, D.K. Ghosh, L.J. Roman, P. Martasek, J.C. Salerno, Thermodynamics of oxidation-reduction reaction in mammalian nitric oxide synthase, J. Biol. Chem. 279 (2004) 1859–18766.
[49] E.E. Di Ioro, Protein dynamics, FEBS Lett. 307 (1992) 14–19.
[50] A.C. Young, R.F. Tilton, J.C. Dewan, Thermal expansion of hen egg-white lysozyme. Comparison of the 1.9 Å resolution structures of the tetragonal form of the enzyme at 100 K and 298 K, J. Mol. Biol. 235 (1994) 302–317.
[51] F. Parak, H. Hartmann, K.D. Aumann, H. Reuscher, G. Rennekamp, H. Bartunik, W. Steigemann, Low temperature X-ray investigation of structural distributions in myoglobin, Eur. Biophys. J. 15 (1987) 237–249.
[52] J.P. Schelvis, V. Berka, G.T. Babcock, A.L. Tsai, Resonance Raman detection of the Fe—S bond in endothelial nitric oxide synthase, Biochemistry 41 (2002) 5695–5701.